Supplementary Information for

"Selenium isotopes as tracers of a late volatile contribution to Earth from the outer Solar System"

Supplementary Notes

S1 Sample description

Detailed sample information is summarized in Supplementary Table S1. Nine spinel-bearing mantle peridotites from different post-Archean settings and localities including the Pyrenean and Ronda orogenic massifs and the Lanzo and External Ligurides transitional massifs were analyzed in this study. We have also included two peridotite xenoliths hosted by Cenozoic alkali basalts from the French Massif Central (FMC) to cover a wider range of tectonic settings and ages. The incorporation of Ronda, Pyrenees and External Ligurides massifs to the subcontinental lithospheric mantle (SCLM) has been dated as Mid-Proterozoic on the basis of whole-rock Os model ages[48,49]. According to Nd model ages, the northern and central part of the Lanzo massif (sampled by peridotite L212) were isolated from the convective mantle in the late Proterozoic/early Palaeozoic[50]. Selected xenoliths come from the southern part of the FMC, interpreted as SCLM accreted or rejuvenated during the Variscan orogeny[51].

Most of the selected peridotites have been extensively studied for their major and trace element compositions, including platinum-group element[23,24,47,52-57] (Supplementary Table S1), and Se abundances [5,16,22,44,47] (Supplementary Table S2). Exception is sample 15/EDL-007, for which we provide the whole-rock major and trace element data in Supplementary Table S4. These samples cover a wide range of rock texture, mineralogy and geochemical features usually

reported for mantle rocks. Samples mostly from the Pyrenees comprise LREE-depleted, amphibole-free, coarse-granular to mylonitic fertile orogenic lherzolites (TUR 7, FONB 93, 84-1, 15 EDL-007, LiX) along with a highly refractory harzburgite (64-3). All these rocks are devoid of modal metasomatism features apart from minor pargasite in 84-1. Three other orogenic peridotites display clear evidence of melt-rock interactions: L212 (Lanzo), a cpx-poor lherzolite, displays selective enrichment in LREE over HREE interpreted as produced by chromatographic fractionation of a percolating melt [50]. The two Ronda lherzolites are from the fine-granular domain of the Ronda peridotite massif that was affected by pervasive porous melt flow[58]. DR-29 is an olivine-rich "secondary" lherzolite resulting from melt/rock reactions at increasing melt mass. Moreover, it contains abundant disseminated Ti pargasite. DR 33 is an amphibole-free cpx-poor lherzolite showing abundant euhedral Cr spinel and secondary cpx, which were precipitated by melt-rock reaction at decreasing melt volume. The two French Massif Central xenoliths are a coarse-granular LILE and LREE enriched lherzolite with secondary phases (5SC30) and a depleted lherzolite (EG3)[23,24].

Selected peridotites show no correlation with petrogenetic indicators of melt depletion/metasomatism such as Al_2O_3 contents (Fig. 1b), or Pd/Ir ratios, considered sensitive tracers of refertilization and metasomatic processes affecting the HSEs and Se-Te systematics[16,59] (Supplementary Figure S1), further supporting that partial melting and metasomatism do not produce a Se isotopic variation in mantle peridotites.

S2 Reproducibility and accuracy of Se measurements

Accuracy of Se concentration analyses was checked against the USGS reference material BHVO-2 (Hawaiian basalt). We report an average value of 170 ± 4 ng g^{-1} Se (n = 4) in agreement with previously published values[20,44,60] (Supplementary Table S2). Reproducibilities of Se

concentration measurements estimated from at least 4 replicate analyses of peridotites were better than ~3% r.s.d. (Supplementary Table S2), similar to the long-term analytical reproducibility of 3% r.s.d. reported by Yierpan, et al. [20] in different reference materials.

The long-term analytical reproducibility of Se isotope measurements is 0.07‰ based on multiple analyses of the inter-laboratory standard solution MH-495 (Supplementary Table S3). In addition, the analytical reproducibility obtained from peridotite samples analyzed multiple times ($n \geq 5$) is 0.10‰ (see Methods and Supplementary Table S2). An exception is harzburgite 64-3, with a relatively poor reproducibility of ± 0.20‰ (2 s.d., n=3) that may be attributed to sample heterogeneity or to measurement-related uncertainties such as low signals on ^{82}Se. For this particular sample, it has been shown that heterogeneity plays an important role in its Se concentration reproducibility, where the more material was digested, the better the reproducibility[44]. Although in our case the Se concentration reproducibility is 3% r.s.d. (Supplementary Table S2), the depleted Se content (Se= 5.79 ± 0.17 ng g^{-1}, Supplementary Table S2) may contribute to the poor reproducibility of its Se isotopic composition. On the other hand, internal errors (s.e.) of Se isotope measurements are inversely correlated with the measured signals on ^{82}Se and with the amount of Se analyzed (Supplementary Table S2, Supplementary Figure S2). These correlations show that analyses of low Se contents (~7 ng of Se) have the highest internal errors (up to 0.11‰, 2 s.e.; Supplementary Table S2), as also described by Kurzawa, et al. [21] and which may result in poor reproducibility of the $\delta^{82/76}$Se measurements. However, no apparent correlation is observed between the measured signals on ^{82}Se (as low as 0.2 V) or the amount of Se analyzed and the $\delta^{82/76}$Se of the samples (Supplementary Table S2, Supplementary Figure S2).

No high-precision Se isotopic data have been published for peridotites following the pioneering study of Rouxel, et al. [27], who provided the first Se isotopic value for the USGS

reference peridotite (PCC-1) and for the BSE (Fig. 2). Thus, we performed an accuracy test for the type of peridotite-matrix analyzed here, already tested in standard solutions[21] and previously used for testing other isotope systems[61,62]. Increasing amounts of the fertile lherzolite TUR 7 (from ~5 to 50 ng of Se) were admixed to a constant amount of MH-495 reference material (~10 or 200 ng of Se) (Supplementary Table S5). Each mixture was then spiked accordingly to its Se concentration and processed as a normal sample. The measured $\delta^{82/76}$Se of the mixtures are positively correlated with the fraction of Se from TUR 7, forming a mixing line between the $\delta^{82/76}$Se of the end members TUR 7 and MH-495 (r^2= 0.99) and remaining within maximum uncertainty of 0.14‰ (Supplementary Figure S3). These results demonstrate that we can discard potential bias induced by peridotite-matrix or interferences during analysis.

S3 Potential mixtures between chondrite-like material

a) Mixtures between CM chondrites Murchison and Mighei

A potential mixture between the CM chondrites Murchison and Mighei could result in a Se isotope signature that fits with that of the BSE. To calculate the possible range of mixtures we use the following mass balance equation:

$$\frac{f \times C_1 \times \delta^{82/76}Se_1 + (1-\mathrm{f}) \times C_2 \times \delta^{82/76}Se_2}{f \times C_1 + (1-f) \times C_2} = \delta^{82/76}Se_{BSE} \qquad \text{(Eq.1)}$$

f : Fraction of Murchison in the mixture
$1 - f$: Fraction of Mighei in the mixture
C_1: Se concentration of Murchison (µg/g)
C_2: Se concentration of Mighei (µg/g)
$\delta^{82/76}Se_1$: Se isotope signature of Murchison (‰)
$\delta^{82/76}Se_2$: Se isotope signature of Mighei (‰)
$\delta^{82/76}Se_{BSE}$: Se isotope signature of BSE from this study (‰)

Se concentrations of Murchison (12.7 ± 0.8 µg g^{-1}) and Mighei (24.3 ± 1.4 µg g^{-1}) and their respective $\delta^{82/76}$Se values (0.20 ± 0.13‰ and -0.30 ± 0.10‰) used in the equation are from Labidi, et al. [19]. Our calculations result in a *f* value, fraction of Murchison in the mixture, that ranges between 0.49 and 0.89 (*f*= 0.69 ± 0.20) and thus allows for proportional contributions from Mighei that range between 0.11 and 0.51. The uncertainty was calculated by propagating the errors associated with the concentration of Se in both chondrites (Supplementary Table S6) and the uncertainties of the $\delta^{82/76}$Se values[19].

b) Potential mixtures of CI and different types of chondrite-like material

Potential mixtures between CI and different types of chondrite-type material might also account for the Se isotope composition of the BSE. Following Eq. 1, we calculate mixtures between CI and CO, CV, each sub-type of CM (Mighei and Murchison), ordinary and enstatite chondrites that would result in a Se isotope signature that fits with that of the BSE (Supplementary Table S7). Our calculations show that for all potential mixtures, the average contribution from a CI chondrite-like material is always higher than 85%, and in most cases higher than 90% (CI-Enstatite; CI-Murchison and CI-Mighei), clearly indicating that carbonaceous chondrites dominated the late-accreted material. The uncertainty for each mixture was calculated by propagating the errors associated with the concentration of Se in both components (Supplementary Tables S6 and S7) and the uncertainties of the $\delta^{82/76}$Se values[19].

S4 Mass of the late veneer and its contribution to the volatile budget of the BSE

To calculate the mass of the late veneer we considered that ~40% of S is in the pre-late veneer mantle[30] and use a BSE S content of 200 ± 40 µg/g[31]. To obtain the percentage of the Earth's mass added to the BSE by a CI or CM chondrite-like late veneer ('a' term) we use the same mass balance approach than in the mixture of chondrite material (see above):

$$C_{BSE}^{X} \times M_{BSE} = C_{CC}^{X} \times a \times M_E + C_{PLV}^{X} \times (M_{BSE} - a \times M_E) \qquad \text{Eq.2}$$

C_{BSE}^{X}: Concentration of element X in the BSE
C_{CC}^{X}: Concentration of element X in the chondrite
C_{PLV}^{X}: Concentration of element X in the pre-late veneer mantle
a: Percentage of the Earth's mass added to the BSE by the late veneer
M_{BSE}, M_E: mass of the BSE and the Earth from [31, and references therein]

Abundances (± s.d.) of CI and CM chondrite elements used in Eq. 2 are reported in Supplementary Table S6[5,18-19,60,63]. Our results show that 0.15 ± 0.03% of the Earth's mass would be added by a CI chondrite-like late veneer, which is lower than the 0.26 ± 0.05 % resulting if we consider CM chondrite-like late veneer. The associated uncertainties in both calculations were calculated by propagating the errors associated with the concentration of S, Se and $\delta^{82/76}$Se, both in the BSE and chondrites (CI or Murchison and Mighei mixture; Supplementary Table S6). More complex scenarios involving mixtures of CI and different types of chondrite-type material (c.f. S3b) would result in a late veneer of 0.15-0.16% the Earth's mass. Abundances (± s.d.), fractions and estimated late veneer mass of potential mixtures are reported in Supplementary Table S7.

Since the late veneer delivered 100% of Se and Te based on their partition coefficients[9], a CI chondrite-like late veneer would result in Se and Te BSE abundances of 47 ± 9 and 5 ± 1 ng g^{-1}, respectively (Supplementary Table S6). These BSE estimates are within error of those obtained assuming a CM chondrite-like late veneer (Se = 65 ± 17 ng g^{-1}; Te= 6 ± 1 ng g^{-1}; Supplementary Table S6). Our results imply Se and Te BSE abundances lower than previous estimates based on Se and Te contents and relative proportions in mantle fertile lherzolites (~80 ng g^{-1} of Se and ~11 ng g^{-1} of Te)[5,6,31]. It has been shown however that Se-Te systematics in peridotites might not be

representative of the BSE and instead represent the result of refertilization and metasomatic processes[16,17].

Regarding other elements such as water, carbon and nitrogen, the contribution of the late veneer would have been heterogeneous and it relies on how well constrained are the estimate BSE abundances of these elements (Supplementary Table S6). Following Palme and O'Neill [31] water content in the BSE, a CI chondrite-like late veneer would have provided either ~20-40% of water if the Earth has chondritic refractory lithophile element ratios, i.e. a water abundance of 1100 ± 220 μg g^{-1}, or ~30-60% of water if Earth is non-chondritic (BSE water of 675 ± 135 μg g^{-1}). Similarly, a CM chondrite-like late veneer would have delivered either ~25-45% or ~40-70% of water assuming a chondritic or a non-chondritic model, respectively. Hirschmann [64] constrained the carbon content in the BSE, providing two different estimates of 90 ± 27 μg g^{-1} and 108 ± 34 μg g^{-1}. According to those estimates, a CI chondrite-like late veneer would have delivered ~57-120% or ~46 – 100% of the BSE carbon, respectively, whereas a CM chondrite-like late veneer would have delivered ~60-130% or ~50 – 110%. These estimates imply that a CI or CM chondrite-like late veneer could have delivered more than 100% of the BSE carbon. Recent studies, however, have suggested that ~10-30% of the present day carbon budget corresponds to pre-late veneer mantle abundances[39], which supports that the late veneer delivered ~80% of the BSE carbon budget, in agreement with the average values provided by our calculations. Nitrogen abundance in the BSE (1.9 ± 0.37 μg g^{-1}, [65]) is much lower than the calculated amounts delivered by the late veneer (CI chondrite contribution: 4.3 ± 1.1 μg g^{-1}; CM chondrite contribution: 3.8 ± 1.8 μg g^{-1}; Supplementary Table S6). However, the excess nitrogen abundance (CI chondrite contribution: between 120 to 320%; CM chondrite contribution: between 80 to 320%) can be reconciled with considerable atmospheric loss [41] after the late veneer. This does not preclude that nitrogen was already in the mantle previous to the late veneer.

Supplementary Table Captions

Supplementary Table S1.

Details on rock types, localities, Al_2O_3 content and Pd_N/Ir_N ratios of selected peridotites.

Supplementary Table S2.

Detailed information about the Se data obtained per sample measurement together with published data.

Supplementary Table S3.

The $\delta^{82/76}$Se value of the inter-laboratory standard MH 495 (30 ng mL^{-1} Se) measured together with the samples in this study and previously reported

Supplementary Table S4.

New major and trace element data for peridotite 15/EDL-007.

Supplementary Table S5.

Se isotope data of mixtures between MH-495 standard and peridotite TUR-7.

Supplementary Table S6.

Recent estimates of the volatile content of carbonaceous chondrites and the BSE, together with the estimated contribution of a CI and CM chondrite-like late veneer.

Supplementary Table S7.

Summary of potential mixtures between CI chondrite-like material and different types of chondrites that could result in a Se isotope signature that would overlap that of the BSE.

Supplementary Figures

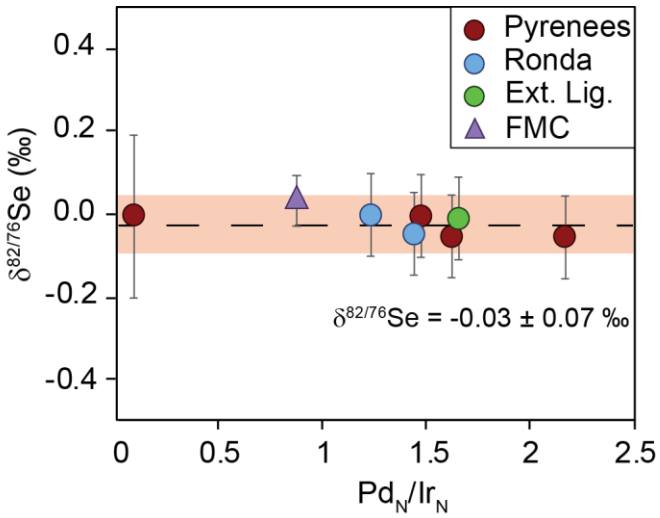

Supplementary Figure S1. Pd_N/Ir_N vs. Se isotope data of mantle peridotites.

Circles represent orogenic and transitional peridotites and triangles mantle xenoliths. N = CI-chondrite normalized [31]. Error bars indicate 2 s.d. uncertainties of more than two combined measurements. If not available, the analytical uncertainty obtained for repeated analyses of peridotites is reported (± 0.10‰, 2s.d.) (see Methods). The shaded field represents the 2 s.d. of the mean of peridotites as discussed in the text. Pd and Ir concentrations are taken from published data using the same pulverized powder batch (Supplementary Table S1).

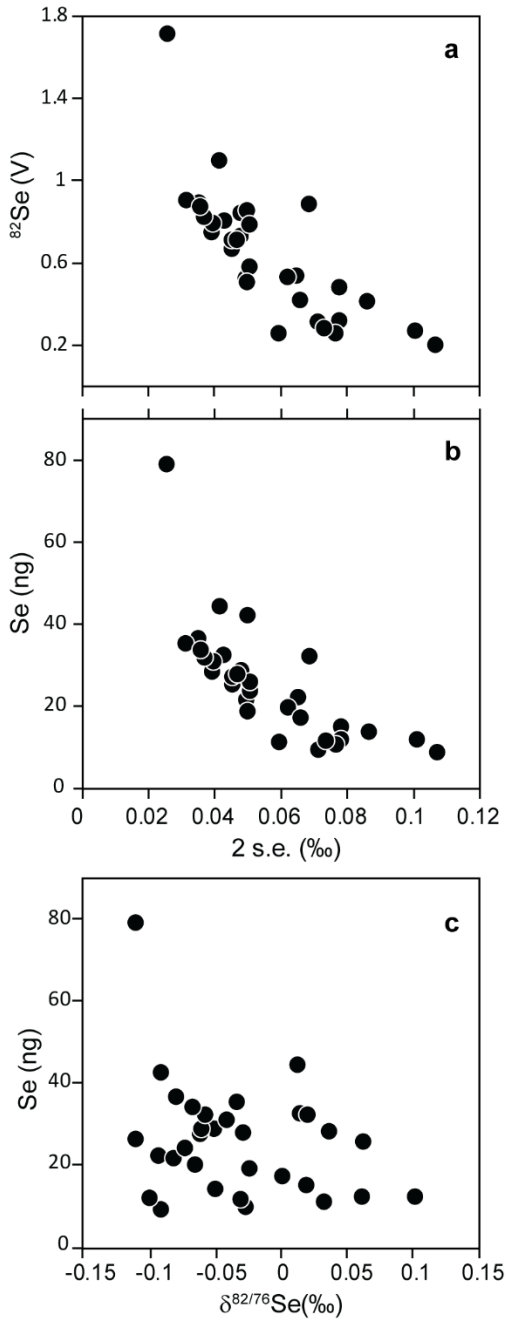

Supplementary Figure S2. Data obtained during Se isotope measurements of peridotites.

Internal errors (s.e.) vs. (a) measured signals on ^{82}Se and (b) amount of Se analyzed. (c) $\delta^{82/76}$Se (‰) vs. the amount of Se analyzed (Supplementary Table S2).

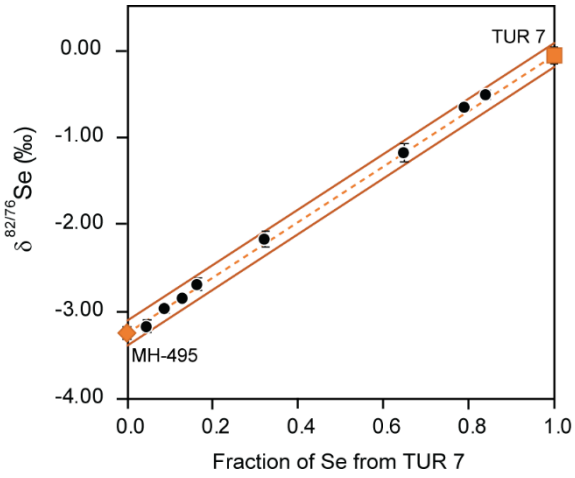

Supplementary Figure S3. Accuracy test. $\delta^{82/76}$Se (‰) values of the mixture between a constant amount of the standard solution MH-495 (~10 or 200 ng of Se) and different amounts of the fertile lherzolite TUR 7 (from ~5 to 50 ng of Se) vs. the fraction of Se from TUR 7. Error bars represent the internal precision of sample measurement reported as 2 s.e. (Supplementary Table S5). The doped samples fall on the range defined by the Se isotope compositions of the end members MH-495 ($\delta^{82/76}$Se = -3.25 ± 0.07 ‰, Supplementary Table S3) and TUR 7 ($\delta^{82/76}$Se = -0.06 ± 0.10 ‰; Supplementary Table S2) and remain within maximum uncertainty of 0.14‰ (2 s.d.).

Supplementary References

48 Reisberg, L. & Lorand, J. P. Longevity of sub-continental mantle lithosphere from osmium isotope systematics in orogenic peridotite massifs. *Nature* **376**, 159-162 (1995).

49 Snow, J. E., Schmidt, G. & Rampone, E. Os isotopes and highly siderophile elements (HSE) in the Ligurian ophiolites, Italy. *Earth and Planetary Science Letters* **175**, 119-132 (2000).

50 Bodinier, J.-L., Menzies, M. A. & Thirlwall, M. F. Continental to Oceanic Mantle Transition—REE and Sr-Nd Isotopic Geochemistry of the Lanzo Lherzolite Massif. *Journal of Petrology* **Special_Volume**, 191-210 (1991).

51 Lenoir, X., Garrido, C., Bodinier, J. & Dautria, J. Contrasting lithospheric mantle domains beneath the Massif Central (France) revealed by geochemistry of peridotite xenoliths. *Earth and Planetary Science Letters* **181**, 359-375 (2000).

52 Lorand, J.-P., Pattou, L. & Gros, M. Fractionation of Platinum-group Elements and Gold in the Upper Mantle: a Detailed Study in Pyrenean Orogenic Lherzolites. *Journal of Petrology* **40**, 957-981 (1999).
53 Luguet, A., Shirey, S. B., Lorand, J.-P., Horan, M. F. & Carlson, R. W. Residual platinum-group minerals from highly depleted harzburgites of the Lherz massif (France) and their role in HSE fractionation of the mantle. *Geochimica et Cosmochimica Acta* **71**, 3082-3097 (2007).
54 Van der Wal, D. & Bodinier, J. L. Origin of the recrystallisation front in the Ronda peridotite by km-scale pervasive porous melt flow. *Contributions to Mineralogy and Petrology* **122**, 387-405 (1996).
55 Lorand, J. P., Keays, R. R. & Bodinier, J. L. Copper and Noble Metal Enrichments Across the Lithosphere—Asthenosphere Boundary of Mantle Diapirs: Evidence from the Lanzo Lherzolite Massif. *Journal of Petrology* **34**, 1111-1140 (1993).
56 Becker, H. *et al.* Highly siderophile element composition of the Earth's primitive upper mantle: Constraints from new data on peridotite massifs and xenoliths. *Geochimica et Cosmochimica Acta* **70**, 4528-4550 (2006).
57 Luguet, A., Lorand, J.-P., Alard, O. & Cottin, J.-Y. A multi-technique study of platinum group element systematic in some Ligurian ophiolitic peridotites, Italy. *Chemical Geology* **208**, 175-194 (2004).
58 der Wal, D. V. & Bodinier, J. L. Origin of the recrystallisation front in the Ronda peridotite by km-scale pervasive porous melt flow. *Contributions to Mineralogy and Petrology* **122**, 387-405 (1996).
59 Luguet, A., Behrens, M., Pearson, D. G., König, S. & Herwartz, D. Significance of the whole rock Re–Os ages in cryptically and modally metasomatised cratonic peridotites: Constraints from HSE–Se–Te systematics. *Geochimica et Cosmochimica Acta* **164**, 441-463 (2015).
60 Wang, Z., Becker, H. & Wombacher, F. Mass Fractions of S, Cu, Se, Mo, Ag, Cd, In, Te, Ba, Sm, W, Tl and Bi in Geological Reference Materials and Selected Carbonaceous Chondrites Determined by Isotope Dilution ICP-MS. *Geostandards and Geoanalytical Research* **39**, 185-208 (2015).
61 Nielsen, S. G., Rehkämper, M., Baker, J. & Halliday, A. N. The precise and accurate determination of thallium isotope compositions and concentrations for water samples by MC-ICPMS. *Chemical Geology* **204**, 109-124 (2004).
62 Tipper, E. T., Louvat, P., Capmas, F., Galy, A. & Gaillardet, J. Accuracy of stable Mg and Ca isotope data obtained by MC-ICP-MS using the standard addition method. *Chemical Geology* **257**, 65-75 (2008).
63 Braukmüller, N., Wombacher, F., Hezel, D. C., Escoube, R. & Münker, C. Ta. *Geochimica et Cosmochimica Acta* **239**, 17-48 (2018).
64 Hirschmann, M. M. Constraints on the early delivery and fractionation of Earth's major volatiles from C/H, C/N, and C/S ratios. *American Mineralogist* **101**, 540-553 (2016).
65 Marty, B. & Dauphas, N. The nitrogen record of crust–mantle interaction and mantle convection from Archean to Present. *Earth and Planetary Science Letters* **206**, 397-410 (2003).